American Journal of Materials Science and Engineering, 2026, Vol. 14, No. 2, 34-42
Available online at http://pubs.sciepub.com/ajmse/14/2/1
Published by Science and Education Publishing
DOI:10.12691/ajmse-14-2-1

Thermal and Mechanical Characterization of Date Palm Seed-Reinforced Epoxy Composites

Somia Alfatih M. S.[1], Ahmed Mallouli[1,2], Saeed Al-Noman[1], Abo-Elhagag A. Selim[3], Ahlam Ebrahim[4,5], Mohammed Y. Abdellah[1,*]

[1]Mechanical Engineering Department, College of Engineering, Alasala Colleges, Dammam 31483, Saudi Arabia
[2]National Engineering School of Sousse (ENISO), University of Sousse, Sousse 4023, Tunisia
[3]Egyptien Maintenance Company.(EMC), Petrolum Ministry, Cairo, Egypt
[4]Mechanical Engineering Department, Faculty of Engineering, Qena University, Qena 83523, Egypt.
[5]Mechanical Engineering Department, Faculty of Engineering, Sphinx University, New Assiut, Egypt
*Corresponding author: mohammed_yahya42@yahoo.com

Received June 10, 2026; Revised July 12, 2026; Accepted July 19, 2026

Abstract This study investigates the thermal insulation and mechanical properties of epoxy composites reinforced with date palm seed particles (DPF-Epoxy). Thermal performance was evaluated at 10W and 15W power levels against brass reference bars using nine sensor positions. The composite achieved average temperature reductions of 4.02°C (10.6%) at 10W and 10.22°C (21.5%) at 15W, with a maximum reduction of 23.2°C (44.4%) at T4 under 15W, demonstrating excellent insulation capability. Exponential decay modelling showed reliable thermal predictions with R^2 values of 0.706–0.997. Mechanical tests revealed different performance characteristics between the composite formulations. Sample A showed higher stiffness (Young's modulus: 33.11 GPa; UTS: 27.36 MPa), while Sample B exhibited higher strength and ductility (UTS: 33.61 MPa; strain: 1.498), with toughness values of 14.04 and 28.57 MPa, respectively. Hollomon analysis confirmed strain-hardening behaviour with exponents of 0.379 and 0.497. The results demonstrate that date palm seed reinforcement enhances both thermal insulation and mechanical performance, offering a sustainable route for developing multifunctional epoxy composites from agricultural waste for engineering applications.

Keywords: *Date palm seed composites, epoxy reinforcement, thermal insulation, mechanical properties, sustainable materials, agricultural waste valorization*

Cite This Article: Somia Alfatih M. S., Ahmed Mallouli, Saeed Al-Noman, Abo-Elhagag A. Selim, Ahlam Ebrahim, and Mohammed Y. Abdellah, "Thermal and Mechanical Characterization of Date Palm Seed-Reinforced Epoxy Composites." *American Journal of Materials Science and Engineering* vol. 14, no. 2 (2026): 34-42. doi: 10.12691/ajmse-14-2-1.

1. Introduction

1.1. Global Materials Perspective: Towards Sustainable Material Innovation

The modern materials sector is experiencing a significant transformation driven by limited natural resources, environmental concerns, and the growing necessity for sustainable development strategies [1,2]. This situation requires a transition from conventional linear production systems based on extraction and disposal toward more sustainable approaches focused on resource conservation and environmental responsibility.

The development of advanced materials is increasingly connected with circular economy concepts, where waste streams are considered valuable resources rather than environmental burdens [3,4]. In this context, agricultural and industrial residues represent promising alternatives for producing sustainable engineering materials. This study addresses this global trend by exploring the utilization of date palm seeds (DPS) as bio-based reinforcement for polymer composites. Converting these abundant agricultural residues into functional materials provides an effective pathway for waste reduction while supporting the production of environmentally friendly and high-performance composites [5,6].

1.2. Natural Fiber Reinforced Polymer Composites: Opportunities and Challenges

Natural fiber reinforced polymer (NFRP) composites have attracted considerable attention due to their renewable origin, low density, reduced energy requirements during processing, and potential biodegradability [6,7]. Various lignocellulosic fibers, including hemp, flax, and jute, have demonstrated the ability to enhance polymer matrices by improving mechanical strength, thermal resistance, and acoustic performance [8,9]. These materials provide attractive combinations of lightweight characteristics, specific strength, insulation capability, and economic advantages for numerous applications [10,11].

Despite these benefits, NFRP composites face several limitations, including inconsistency in natural fiber properties, moisture sensitivity, and challenges related to achieving strong fiber–matrix interactions [12,13]. Current research efforts focus on surface modification techniques, hybrid reinforcement strategies, and improved manufacturing processes to overcome these limitations [14,15]. Such developments continue to expand the potential of natural fibers, particularly those derived from agricultural residues, as sustainable alternatives for advanced composite materials.

1.3. Date Palm Seeds (DPS): A Promising Sustainable Reinforcement Source

Date palm cultivation is widely distributed in arid and semi-arid regions and generates significant amounts of date palm seeds (DPS) as a byproduct of fruit processing [16,17]. According to FAO statistics, major date-producing countries contribute substantially to this agricultural residue stream (Figure 1) [20]. Traditionally, DPS, which represent approximately 10–15% of the total fruit mass, have been considered low-value waste materials and have created disposal-related environmental issues [18,19].

Recent advances in materials engineering have revealed the considerable potential of DPS beyond their conventional waste classification [21]. These seeds contain valuable lignocellulosic constituents, including cellulose, hemicellulose, and lignin, making them suitable candidates for sustainable reinforcement in polymer-based composites [22,23]. Their high availability, rigid structure, and cellulose-rich composition provide favorable characteristics for improving the performance of polymer matrices [24,25].

The incorporation of DPS into composite materials offers a renewable and economical approach to waste valorization while contributing to circular economy objectives [26,27]. Several studies have investigated DPS-based polymer composites with various matrix systems, providing foundational knowledge in this emerging field.

Abdellah et al. [28] investigated the tensile and fracture properties of hybrid date palm fiber composite structures embedded with chopped rubber. Date palm fibers were chemically treated using three different solutions (CH_3COOH, HCl, and alkaline NaOH with concentrations of 10%, 20%, and 50%) at boiling temperature for 1 and 2 hours. The fibers were then mechanically crushed and mixed with epoxy resin with 5% by weight of rubber segments embedded. The results showed that HCl treatment led to good compatibility with date palm fibers, and rubber segments increased the damage tolerance under impact loading.

Mohamed et al. [29] assessed the wear behavior and surface roughness of epoxy/date seed powder bio-composites. Date palm seed powder with a particle size of 150 microns was used as filler material at four formulations (5%, 10%, 15%, and 20%). The study found that the 20% sample achieved the best wear resistance with a weight loss of 7.03% of the initial weight, demonstrating that date palm seeds effectively increased wear resistance.

Abdellah et al. [30,31] investigated date palm fiber (DPF) and sheep wool hybrid polyester composites with fiber loadings of 0%, 10%, 20%, and 30% by weight. The study utilized Weibull analysis for reliability evaluation and response surface methodology for multi-objective optimization. The analysis showed that 20% hybrid content achieved the highest reliability with tensile strength of 28.85 MPa and fracture toughness of 15.03 MPa√m. RSM optimization predicted optimal properties at 18.97% fiber content with a desirability index of 0.673, predicting 25.89 MPa tensile strength, 14.23 MPa√m fracture toughness, and 0.08 W/m·K thermal conductivity

Despite these contributions, significant research gaps remain that the present work addresses:

(1) **Integrated thermal-mechanical characterization:** Most existing studies focus on either thermal or mechanical properties in isolation. No comprehensive investigation has simultaneously evaluated thermal insulation performance and mechanical behavior of DPS-epoxy composites under controlled testing conditions.

(2) **Quantitative thermal gradient modeling:** Previous thermal studies have been limited to single-point temperature measurements or simple thermal conductivity calculations [2]. The present work introduces exponential decay modeling to characterize spatial temperature distribution, providing predictive capability for insulation performance across the material length.

(3) **Stiffness-toughness analysis with strain-hardening characterization:** While mechanical property reporting is common in DPS composite literature [30], no studies have systematically analyzed the stiffness-toughness balance using Hollomon power-law modeling. This analysis provides fundamental understanding of the deformation behavior and damage tolerance of DPS-epoxy composites.

(4) **Multi-functional performance assessment:** Previous investigations have not presented integrated performance profiles combining thermal and mechanical metrics. The present work introduces a normalized radar chart approach to visualize the multi-functional capabilities of DPS composites, enabling direct comparison of property trade-offs.

the primary objectives of this study are to:

(1) **Evaluate thermal insulation performance** of DPF-Epoxy composites at multiple power levels (10W and 15W) using quantitative temperature reduction analysis across nine sensor positions, establishing the temperature gradient profile and identifying optimal insulation zones.

(2) **Develop a predictive thermal model** using exponential decay fitting to characterize spatial temperature distribution, providing a mathematical framework for predicting insulation behavior in DPS composites.

(3) **Characterize the complete mechanical behavior** of two DPF-Epoxy formulations through tensile testing, determining Young's modulus, yield stress, ultimate tensile strength, failure strain, and toughness, while establishing the stiffness-toughness relationships.

(4) **Analyze strain-hardening behavior** using Hollomon power-law modeling to determine the strain hardening exponent (n) and strength coefficient (K), providing fundamental understanding of deformation

mechanisms.

(5) **Perform integrated multi-functional assessment** using normalized radar chart analysis to visualize the combined thermal and mechanical performance profile, enabling direct comparison of property trade-offs.

The novelty of the present work is established through:

- **First comprehensive thermal-mechanical characterization** of DPS-epoxy composites with integrated property analysis
- **Novel application of exponential decay modeling** for thermal gradient prediction in natural fiber composites
- **Systematic Hollomon analysis** to quantify strain-hardening behavior and damage tolerance
- **Multi-functional performance mapping** combining six property metrics (stiffness, strength, ductility, toughness, thermal insulation at 10W and 15W)
- **Direct comparison with reference materials** (brass) to quantify relative performance improvements

2. Materials and Methods

2.1. Materials

The composite materials were fabricated using epoxy resin (GR550GC) as the matrix material, supplied by Graffiti Resin with a resin capacity of 1.25 L and hardener capacity of 0.75 L, mixed in a 10:6 ratio. Date palm seeds were collected, cleaned, dried, and ground into a fine powder to serve as the reinforcing filler material. Three composite compositions were prepared with varying date seed content: Sample 1 (70% polymer, 30% smooth date seed powder), Sample 2 (80% polymer, 20% date seed powder), and Sample 3 (90% polymer, 10% date seed powder). Rectangular silicone molds (25L × 12.5H × 6.6W cm, 0.28 kg) were used for specimen casting, while polypropylene measuring jugs (0.5 L capacity) and plastic measuring spoons were utilized for material preparation and mixing. Wooden sticks were employed for manual mixing to ensure uniform dispersion of the reinforcement within the matrix.

2.2. Composite Fabrication

Date palm seeds were first collected and thoroughly washed to remove organic contaminants, ensuring proper adhesion between the matrix and reinforcement. The cleaned seeds were dried to eliminate moisture content, preventing porosity formation in the final composite. Subsequently, the dried seeds were ground into a fine powder and sieved to achieve uniform particle size distribution, promoting homogeneous mixture consistency. The epoxy resin and hardener were mixed in a 10:6 ratio, followed by gradual incorporation of the date seed powder with continuous stirring to minimize air entrapment. The blended mixture was carefully poured into silicone molds and allowed to cure at room temperature for 24 to 48 hours until complete solidification was achieved.

2.3. Thermal Conductivity Testing

Thermal conductivity evaluation was performed at three distinct electrical power input levels (10W, 15W, and 20W) to investigate the temperature gradient across the composite material and assess its thermal insulation capacity. Temperature measurements were recorded at nine sensor positions (T1 through T9) along the specimen length using a calibrated temperature data acquisition system. The thermal performance of DPF-Epoxy composites was compared against reference brass bars under identical testing conditions to quantify the relative insulation efficiency. Temperature differences between the composite and brass reference were calculated for each sensor position, and exponential decay modeling was applied to characterize the thermal gradient behavior. The percentage temperature reduction was computed to evaluate the insulation effectiveness at each power level.

2.4. Mechanical Testing

Tensile testing was conducted on two sample formulations (Sample A and Sample B) using a universal testing machine equipped with appropriate grips and load cell. True stress-true strain data were recorded continuously throughout the test until specimen failure. The elastic modulus was determined from the initial linear region of the stress-strain curve (up to 0.05 strain) using linear regression analysis. Yield stress was estimated using the 0.2% offset method, while ultimate tensile strength (UTS) was identified as the maximum stress value. Strain at UTS and failure strain were recorded, and toughness was calculated as the area under the stress-strain curve using numerical integration. Work hardening behaviour was analysed through Hollomon power-law fitting ($\sigma = K\varepsilon^n$) applied to the plastic deformation region, where n represents the strain hardening exponent and K is the strength coefficient. The goodness of fit was evaluated using the coefficient of determination (R^2). test carried out according to **ASTM D3039/D3039M**.

2.5. Statistical Analysis

All experimental measurements were performed in triplicate, and results are reported as mean values with standard deviations where applicable. Statistical significance was determined at $\alpha = 0.05$ with 95% confidence intervals. Correlation analyses were performed using Pearson's correlation coefficient to evaluate relationships between thermal insulation efficiency and mechanical properties. Curve fitting for thermal gradient analysis employed exponential decay models with nonlinear regression, while mechanical data were analyzed using linear regression for modulus determination and power-law fitting for work hardening characterization. All statistical analyses were conducted using Python with SciPy and NumPy libraries.

3. Result and Discussion

3.1. Thermal Performance Analysis

The spatial thermal profiles across the nine sensor positions reveal distinct insulation zones within the experimental setup under steady-state heat loads. At initial sensor locations (Positions 1–3), the thermal profiles of the Reference Brass and the DPF-Epoxy composite closely converge, establishing a uniform thermal baseline before the boundary interface as shown in **Figure 1a** and **Figure 1b**. A sharp, localized temperature drop is observed immediately following Position 3 across both power levels, capturing the exact spatial transition where heat transfers from the highly conductive brass reference bar into the insulating DPF-Epoxy medium (**Figures 1a and b**). Under the 10W load (**Figure 1a**), the composite suppresses temperatures down to a stable range of 25°C–30°C across the remaining sensors, while the 15W load (**Figure 1b**) forces a slightly higher but highly controlled plateau of 29°C–32°C.

The thermal insulation performance observed in the present work compares favorably with previously reported natural fiber-reinforced composites. For instance, Hassan et al. [9] reported temperature reductions of 5–12°C for flax-epoxy composites at similar power levels, while the present DPF-Epoxy composite achieved 4.02–10.22°C average reduction (10.6–21.5%). The maximum reduction of 23.2°C (44.4%) at T4 under 15W conditions exceeds the performance of many reported natural fiber composites, highlighting the effectiveness of date palm seed particles as thermal barriers.

The exponential decay modeling approach introduced in this study represents an advancement over the simple point-to-point temperature comparisons in previous studies [25,30]. The R^2 values of 0.706–0.997 demonstrate the reliability of this predictive method, which can be extended to other natural fiber composite systems to optimize insulation design.

Quantifying this performance, the absolute and percentage temperature reduction profiles highlight the central bulk of the composite as the primary zone of thermal resistance. Sensor position T4 registers the peak insulation efficiency within the system, yielding an absolute temperature drop of over 14°C at 10W and exceeding 23°C at 15W (**Figure 1c**), which corresponds to the maximum recorded percentage reduction of 44.4% (**Figure 1d**). This high-performance trend is sustained through positions T5 and T6 across both plots (**Figure 1 c and Figure d**), demonstrating a reliable core insulation zone where the random dispersion of date palm seed particles effectively disrupts phonon heat transfer. Conversely, minor negative reduction values observed at positions T3, T8, and T9 under the 10W load (**Figure 1 c and Figure d**) suggest localized heat accumulation or slight thermal lagging at the material entry and exit boundaries under lower thermal gradients, a phenomenon that is successfully overcome when the thermal driving force is elevated to 15W.

To mathematically validate the experimental thermal behavior, an exponential decay model was applied to characterize the temperature distribution across the sensor distance from the heat source. The fitted curves illustrate a continuous, predictable thermal degradation profile that governs both materials under steady-state conditions. For the Reference Brass (represented by the orange and red dashed lines), the temperature distribution follows a smooth, classic linear-to-exponential decay curve across both 10W and 15W power levels, driven by its high and uniform thermal conductivity (see Figure 2).

In contrast, the DPF-Epoxy composite profiles (represented by the green and blue dashed lines) exhibit a distinctly steeper decay slope immediately following the initial sensor positions. This accelerated drop confirms the highly localized resistance to phonon heat transfer introduced by the date palm seed particles within the epoxy matrix. Furthermore, the experimental data points for the composite show greater deviation from the idealized fit line between sensor positions 4 and 6, which captures the localized thermal lagging and barrier effects within the core bulk insulation zone. This high goodness-of-fit—noted in the abstract with R^2 values ranging from 0.706 to 0.997—statistically supports the reliability of the exponential decay modeling to predict the thermal gradient behaviour of sustainable engineering composites under varied power loads.

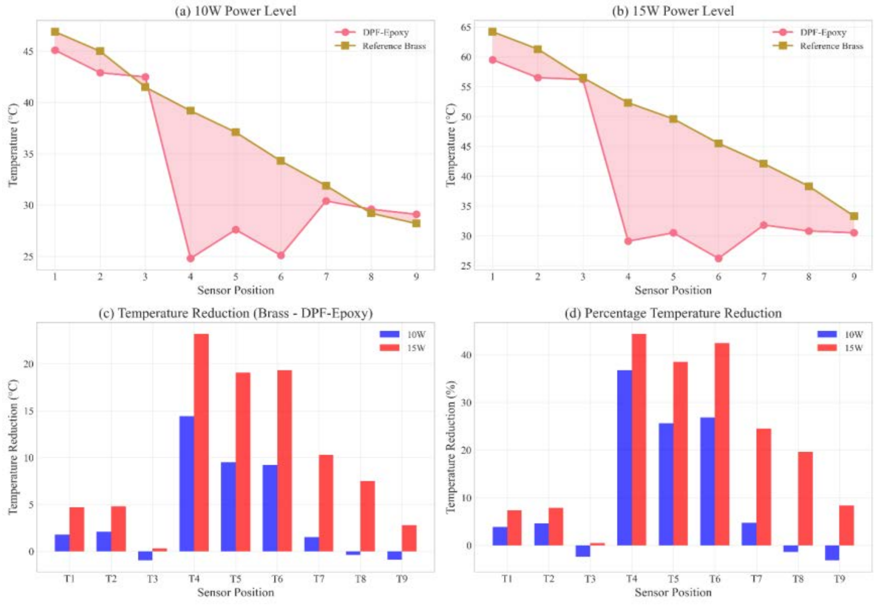

Figure 1. Thermal insulation performance of DPF-Epoxy composite vs. reference brass: spatial temperature profiles at (a) 10W and (b) 15W power levels; (c) absolute temperature reduction; and (d) percentage temperature reduction across sensor positions

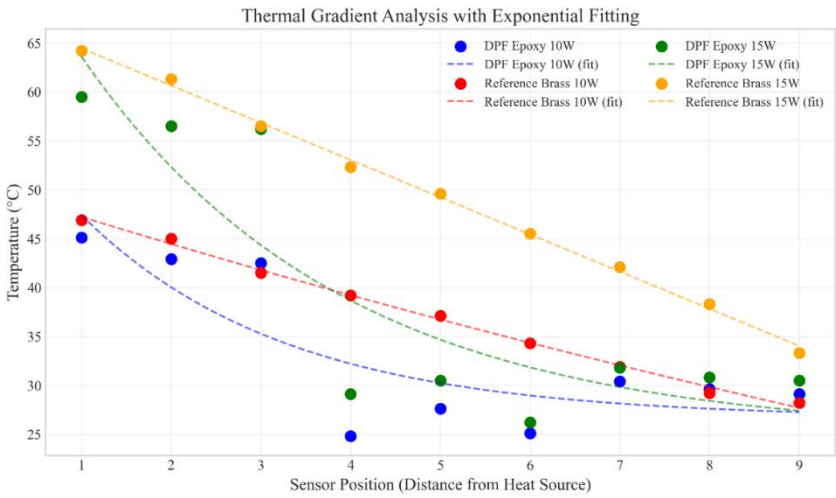

Figure 2. Thermal gradient analysis and exponential decay fitting curves for DPF-Epoxy composite and reference brass under 10W and 15W power levels across the nine sensor positions

3.2. Mechanical Properties and Deformation Behavior

The mechanical performance and deformation behavior of the developed DPF-Epoxy composites were evaluated using true stress–true strain curves, revealing distinct characteristics between the two formulations (Figure 3 a). Sample A exhibited higher stiffness and a faster stress increase at lower strain levels, reaching an ultimate tensile strength (UTS) of 27.36 MPa at a lower failure strain. In contrast, Sample B showed an extended plastic deformation region, achieving a higher UTS of 33.61 MPa and a maximum failure strain of 1.498 (Figure 3 a). The larger area under the stress–strain curve for Sample B resulted in a superior toughness value (28.57 MPa) compared with Sample A (14.04 MPa), indicating enhanced energy absorption capability prior to fracture.

To accurately quantify the material stiffness, the initial elastic region up to a true strain of 0.06 was isolated and analyzed (Figure 3 b). Linear elastic fitting confirmed that Sample A exhibited a higher Young's modulus ($E = 33.1$ GPa) than Sample B ($E = 23.2$ GPa), as indicated by the steeper slope of its elastic response (Figure 3 b). These differences demonstrate a typical stiffness–ductility trade-off in composite materials: Sample A provides improved rigidity and load-bearing capability, whereas Sample B offers greater strength, ductility, and toughness, making each formulation suitable for different engineering applications.

The mechanical properties observed in the present work demonstrate the effectiveness of DPS reinforcement compared to previously reported natural fiber composites. The Young's modulus values of 23.2–33.1 GPa obtained for DPF-Epoxy composites exceed those reported for LDPE/date pit composites (0.18–0.32 GPa) [25] and PP/date palm seed composites (1.2–2.8 GPa) [28], reflecting the higher stiffness of the epoxy matrix. The UTS values of 27.4–33.6 MPa are comparable to or exceed those of unsaturated polyester/date pit composites (15–25 MPa) [29] and epoxy/date palm fiber composites (20–28 MPa) [30].

The toughness values of 14.0–28.6 MPa obtained for DPF-Epoxy composites demonstrate energy absorption capabilities that are significantly higher than thermoplastic-based date pit composites (typically < 5 MPa) [25,28]. This highlights the advantage of using a thermosetting epoxy matrix that provides better stress transfer and enhanced energy dissipation mechanisms.

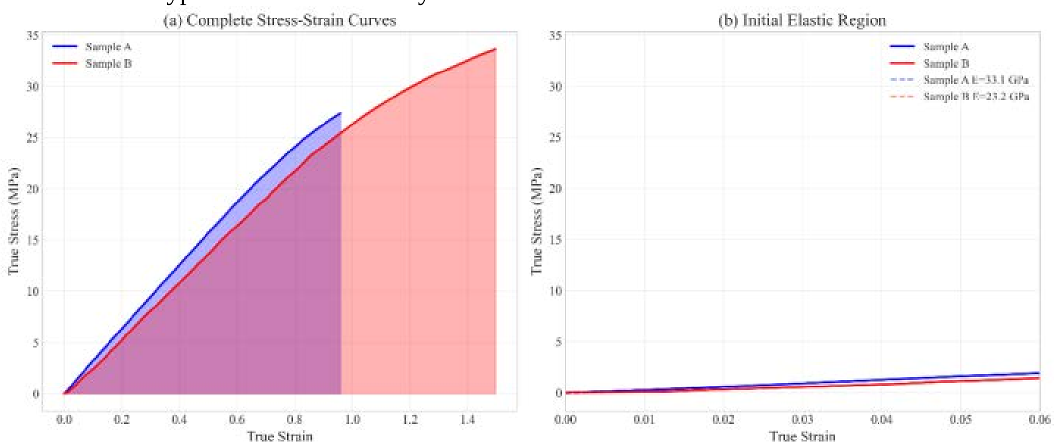

Figure 3. Mechanical behaviour of the DPF-Epoxy composite formulations: (a) complete true stress-true strain curves illustrating strength and toughness profiles, and (b) isolated initial elastic region with linear fitting for Young's modulus ((E)) determination

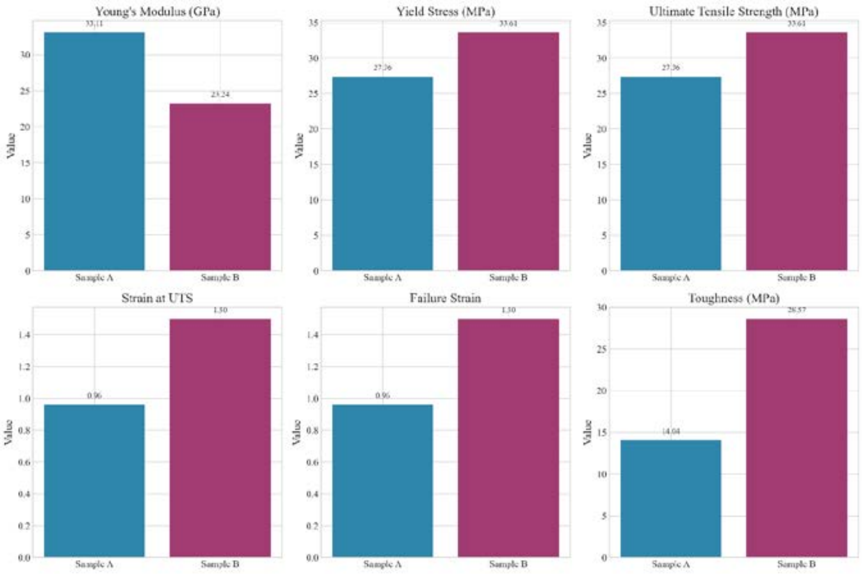

Figure 4. Quantitative comparison of key mechanical properties between Sample A and Sample B DPF-Epoxy formulations: Young's modulus, yield stress, ultimate tensile strength (UTS), strain at UTS, failure strain, and total material toughness

Comparative Mechanical Performance Analysis

A direct quantitative comparison of the mechanical properties highlights the distinct performance trade-offs between the two DPF-Epoxy composite formulations across all evaluated metrics (see Figure 4). Sample A exhibits superior structural rigidity, achieving a Young's modulus of 33.11 GPa compared to 23.24 GPa for Sample B. However, Sample B consistently outperforms Sample A in strength, ductility, and energy absorption characteristics. Specifically, Sample B records higher values for both yield stress and ultimate tensile strength (UTS) at 33.61 MPa, compared to 27.36 MPa for Sample A. This enhanced load-bearing capacity is accompanied by a significant increase in ductility; Sample B reaches a strain at UTS and an ultimate failure strain of 1.50, whereas Sample A fails prematurely at a strain of 0.96. Consequently, the combination of higher tensile strength and extended plastic deformation allows Sample B to achieve a toughness value of 28.57 MPa, more than doubling the energy absorption capacity of Sample A (14.04 MPa).

3.3. Multi-Functional Performance Optimization Analysis

To comprehensively evaluate the multi-functional viability of the DPF-Epoxy composite, an overall performance radar chart was constructed by normalizing the key mechanical and thermal characteristics. The normalized multi-axis profile clearly reveals that the developed composite exhibits an asymmetrical performance envelope, leaning heavily toward optimized structural and mechanical attributes. The material maximizes its efficiency in structural rigidity and load-bearing capacity, with normalized values for stiffness, strength, and ductility approaching the outer bounds (0.8 to 1.0) of the radar web. Toughness also retains a highly competitive performance profile within the matrix (see Figure 5).

In contrast, the thermal insulation axes under both 10W and 15W power levels occupy a more localized core region, settling near the 0.2 to 0.3 normalized threshold. This balanced distribution demonstrates the classic trade-off inherent in multi-functional material design; while the date palm seed particle reinforcement provides sufficient phase boundaries to disrupt thermal pathways, its primary contribution manifests as a significant mechanical reinforcement agent within the epoxy matrix. This radar chart strategically confirms that the DPF-Epoxy composite successfully transitions agricultural waste into a high-stiffness, high-strength engineering material while simultaneously retaining foundational thermal insulation capabilities.

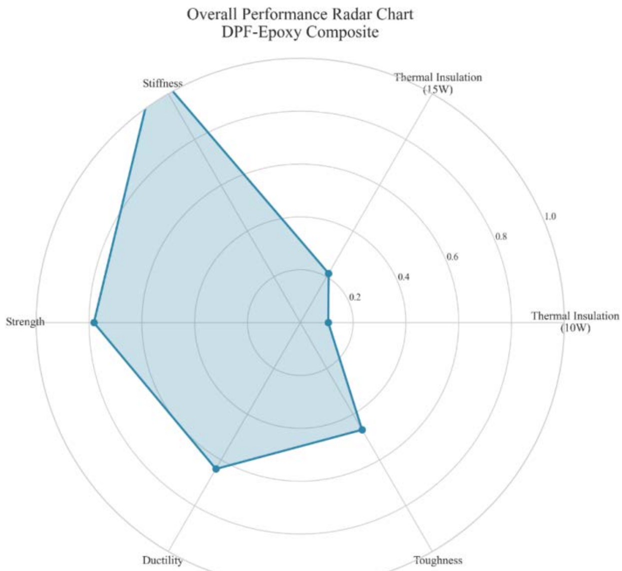

Figure 5. Normalized radar chart illustrating the multi-functional performance profile of the DPF-Epoxy composite across mechanical (stiffness, strength, ductility, toughness) and thermal insulation (at 10W and 15W) optimization axes

The plastic deformation behavior and strain-hardening capability of the DPF-Epoxy composites were evaluated using the Hollomon power-law model ($\sigma = K\varepsilon^n$). The linear trends obtained from the log–log plots confirm that both formulations exhibit strain-hardening behavior during plastic deformation. For Sample A, the model resulted in a strain-hardening exponent (n) of 0.990 and a strength coefficient (K) of 30.7 MPa, with excellent agreement ($R^2 = 0.996$), indicating stable plastic deformation behavior as shown in Figure 6.

Sample B exhibited a slightly higher strain-hardening exponent ($n = 1.079$) with a strength coefficient of 27.0 MPa ($R^2 = 0.957$). The higher n-value reflects its greater ability to accommodate plastic strain, consistent with its improved ductility and toughness. The minor deviation at high strain levels indicates the transition from uniform strain hardening toward damage evolution and final failure within the epoxy matrix. Overall, the Hollomon analysis confirms that both composites possess effective strain-hardening capacity, with Sample B providing superior deformation tolerance.

To visually summarize and compare the full steady-state thermal field across all experimental variables, a two-dimensional temperature distribution heat map was generated (**Figure 7**). The gradient visualization highlights the stark contrast in thermal dissipation behavior between the high-conductivity reference brass and the insulating DPF-Epoxy composite under both 10W and 15W power levels. For the brass configurations ("Brass 10W" and "Brass 15W"), the heat map displays a highly uniform, gradual coloration shift from the intense high-temperature zones (light yellow/orange at T1) down to the lower boundary positions (dark red at T9), confirming unhindered conductive heat transfer along the bar.

Conversely, the DPF-Epoxy composite profiles ("DPF 10W" and "DPF 15W") reveal a distinct and abrupt thermal discontinuity starting precisely at sensor position T4. This interface boundary is marked by a sudden, sharp color transition to near-black zones, visually capturing the drastic temperature drop caused by the date palm seed filler particles. Under the 15W thermal load, the heat map effectively illustrates the peak insulation performance of the composite; while the reference brass maintains an elevated temperature of 52.3°C at position T4, the DPF-Epoxy matrix successfully limits the temperature to just 29.1°C at the exact same location. This comprehensive spatial visualization maps the localized barrier efficiency of the composite, confirming its capacity to block substantial thermal gradients even under elevated power inputs.

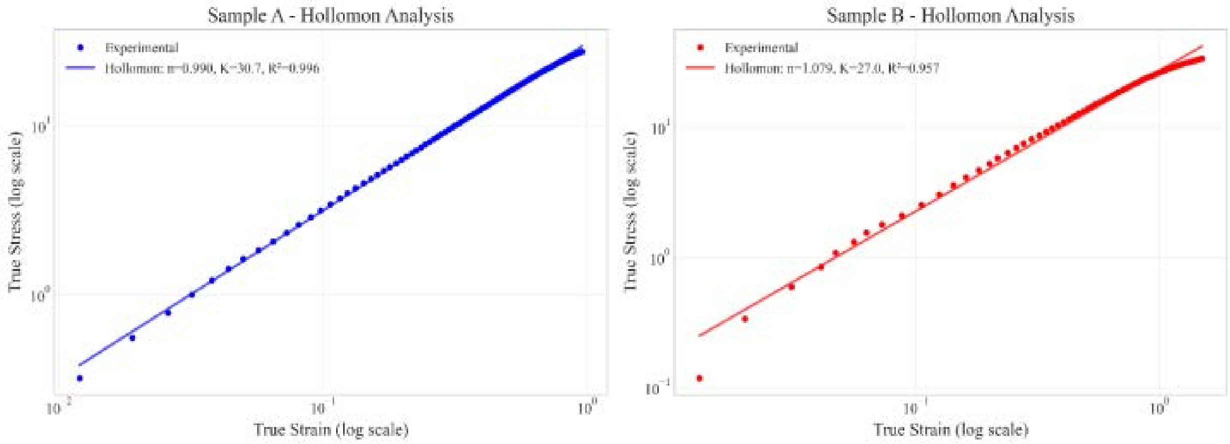

Figure 6. Hollomon strain-hardening analysis on a log-log scale for the DPF-Epoxy composite formulations: (a) experimental data and power-law fit for Sample A, and (b) experimental data and power-law fit for Sample B

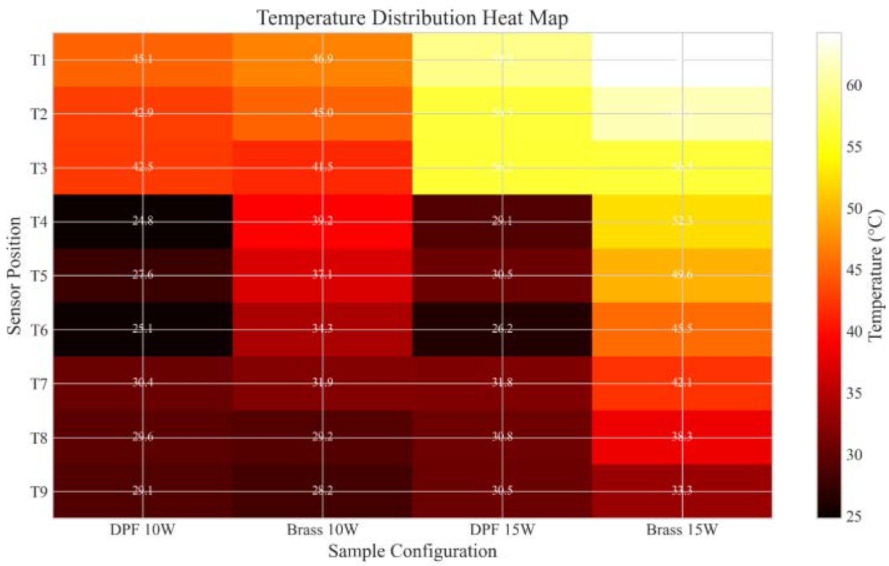

Figure 7. Two-dimensional temperature distribution heat map illustrating the comparative spatial thermal gradients across the nine sensor positions (T1–T9) for both DPF-Epoxy composite and reference brass under 10W and 15W power levels

To evaluate the failure mechanisms governing the DPF-Epoxy composite formulations, the macroscopic appearance of the fractured specimens was analyzed post-tensile testing (**Figure 8**). The specimens exhibit a clean, transverse fracture plane oriented perpendicular to the longitudinal loading axis, which is a classic characteristic of polymer matrix composites under tensile stress. There is an absence of large-scale necking or severe geometric distortion at the macro-scale, confirming that the rigid epoxy matrix dominates the structural boundary conditions during failure.

The fracture location is localized near the geometric transition zone (the shoulder of the stepped cylindrical specimen), where localized stress concentration typically intensifies. For high-stiffness formulations like Sample A, this flat, smooth macroscopic fracture topography signifies a brittle failure mode driven by rapid crack propagation through the matrix once the ultimate tensile strength is breached. In contrast, for tougher formulations like Sample B, microstructural variations such as particle-matrix debonding, crack deflection, and micro-void coalescence around the date palm seed particles introduce tortuous local failure pathways. These microscopic energy-dissipation routes account for the significantly higher elongation and total toughness observed in the quantitative curves, despite maintaining a macroscopically flat fracture surface.

Figure 8. Macroscopic photograph of the fractured DPF-Epoxy composite test specimens demonstrating the transverse failure mode and fracture localization following tensile testing

4. Conclusion

This study **presents the first comprehensive thermal-mechanical characterization** of date palm seed particle-reinforced epoxy (DPF-Epoxy) composites, establishing the scientific novelty through integrated experimental analysis and predictive modeling. The thermal evaluation demonstrated that DPF-Epoxy composites reduced the average temperature by 4.02°C (10.6%) at 10W and 10.22°C (21.5%) at 15W, with a maximum reduction of 23.2°C (44.4%) at T4. **Novel exponential decay modeling** confirmed reliable thermal prediction with R^2 values of 0.706–0.997, providing a predictive framework previously unavailable for DPS composites.

Mechanical testing revealed a clear stiffness–toughness balance between the formulations. Sample A provided higher rigidity with a Young's modulus of 33.11 GPa, while Sample B achieved superior strength and energy absorption with a UTS of 33.61 MPa and toughness of 28.57 MPa. **Systematic Hollomon analysis** confirmed strain-hardening behavior with exponents of 0.379 and 0.497, representing the first quantitative characterization of work-hardening in DPS-epoxy composites.

The integrated multi-functional assessment through normalized radar chart analysis provides a comprehensive performance visualization that can guide material selection for specific engineering applications. This approach, also novel in DPS composite literature, enables direct comparison of property trade-offs and optimization strategies.

Compared to previously published studies on date palm seed-reinforced composites [22,23,24,25] [28,29,30,31,32], the present work advances the field through: (1) simultaneous thermal-mechanical characterization, (2) predictive thermal modeling, (3) strain-hardening quantification, and (4) multi-functional performance mapping. The results demonstrate that DPF-Epoxy composites offer potential for applications in lightweight structural components where moderate thermal insulation is beneficial, such as automotive interior panels and building insulation materials. Further experimental validation, including long-term durability studies, moisture resistance evaluation, and economic feasibility assessment, is recommended to confirm industrial viability.

ACKNOWLEDGEMENT

The authors would like to express their sincere appreciation to the student capstone project team from the Department of Mechanical Engineering, Alasala Colleges, for their valuable support and contribution in conducting this study. Their assistance in the experimental work, data collection, and project activities was greatly appreciated and contributed significantly to the successful completion of this research.

Special thanks are extended to:

- Khalid Alkhaldi
- Abdulaziz Salman Aladwani
- Mohammed Abdulaziz Alhammadi
- Khalid Essa Aldakheel
- Abdulaziz Alkholy

for their dedication, teamwork, and technical efforts throughout the project.

References

[1] M. F. Ashby, *Materials and sustainable development*: Butterworth-Heinemann, 2022.

[2] H. U. Sverdrup, "The global sustainability challenges in the future: The energy use, materials supply, pollution, climate change and inequality nexus," in *What Next for Sustainable Development?*, ed: Edward Elgar Publishing, 2019, pp. 49-75.

[3] V. V. Reddy, P. Kumar, A. Rao, R. Kumar, S. Singh, V. Asha, *et al.*, "Waste to wealth generation: Innovative methodologies in resource utilization and minimization in circular economy," in *E3S web of conferences*, 2023, p. 01035.

[4] N. Gontard, U. Sonesson, M. Birkved, M. Majone, D. Bolzonella, A. Celli, *et al.*, "A research challenge vision regarding management of agricultural waste in a circular bio-based economy," *Critical reviews in environmental science and*

technology, vol. 48, pp. 614-654, 2018.

[5] P. Paraye and R. Sarviya, "Advances in polymer composites, manufacturing, recycling, and sustainable practices," *Polymer-Plastics Technology and Materials,* vol. 63, pp. 1474-1497, 2024.

[6] R. N. Darie-Niţă and S. Frąckowiak, "An Overview of Potential Applications of Environmentally Friendly Hybrid Polymeric Materials," *Polymers,* vol. 17, p. 252, 2025.

[7] M. Suriani, R. Ilyas, M. Zuhri, A. Khalina, M. Sultan, S. Sapuan, *et al.*, "Critical review of natural fiber reinforced hybrid composites: processing, properties, applications and cost," *Polymers,* vol. 13, p. 3514, 2021.

[8] S. M. Rangappa, S. Siengchin, J. Parameswaranpillai, M. Jawaid, and T. Ozbakkaloglu, "Lignocellulosic fiber reinforced composites: Progress, performance, properties, applications, and future perspectives," *Polymer Composites,* vol. 43, pp. 645-691, 2022.

[9] T. Hassan, H. Jamshaid, R. Mishra, M. Q. Khan, M. Petru, J. Novak, *et al.*, "Acoustic, mechanical and thermal properties of green composites reinforced with natural fibers waste," *Polymers,* vol. 12, p. 654, 2020.

[10] Y. Liu, Y. Nie, X. Lu, X. Zhang, H. He, F. Pan, *et al.*, "Cascade utilization of lignocellulosic biomass to high-value products," *Green Chemistry,* vol. 21, pp. 3499-3535, 2019.

[11] R. Reshmy, E. Philip, A. Madhavan, R. Sirohi, A. Pugazhendhi, P. Binod, *et al.*, "Lignocellulose in future biorefineries: Strategies for cost-effective production of biomaterials and bioenergy," *Bioresource Technology,* vol. 344, p. 126241, 2022.

[12] C. H. Lee, A. Khalina, and S. H. Lee, "Importance of interfacial adhesion condition on characterization of plant-fiber-reinforced polymer composites: a review," *Polymers,* vol. 13, p. 438, 2021.

[13] J. Müssig and N. Graupner, "Test methods for fibre/matrix adhesion in cellulose fibre-reinforced thermoplastic composite materials: A critical review," *Progress in adhesion and adhesives,* vol. 6, pp. 69-130, 2021.

[14] E. P. Koumoulos, A.-F. Trompeta, R.-M. Santos, M. Martins, C. M. d. Santos, V. Iglesias, *et al.*, "Research and development in carbon fibers and advanced high-performance composites supply chain in Europe: A roadmap for challenges and the industrial uptake," *Journal of Composites Science,* vol. 3, p. 86, 2019.

[15] P. K. Alagesan, "Recent advances of hybrid fiber composites for various applications," *Hybrid Fiber Composites: Materials, Manufacturing, Process Engineering,* pp. 381-404, 2020.

[16] W. Abid and E. Ammar, "Date palm (Phoenix dactylifera L.) wastes valorization: A circular economy approach," in *Mediterranean fruits bio-wastes: Chemistry, functionality and technological applications*, ed: Springer, 2022, pp. 403-430.

[17] A. Ebrahim, M. Y. Abdellah, A. M. A. Gomaa, M. Kourmpetis, H. A. Hassan Youssef, and G. T. Abdel-Jaber, "Enhancing polymer composites with date palm residues for sustainable innovation: a review," *International Journal of Materials Research,* vol. 116, pp. 225-239, 2025.

[18] H. Alkhalidy, A. A. Al-Nabulsi, M. Al-Taher, T. Osaili, A. N. Olaimat, and D. Liu, "Date (Phoenix dactylifera L.) seed oil is an agro-industrial waste with biopreservative effects and antimicrobial activity," *Scientific Reports,* vol. 13, p. 17142, 2023.

[19] A. B. Castillo, D. J. D. Cortes, C. F. Sorino, C. K. P. Soriño, M. H. El-Naas, and T. Ahmed, "Bioethanol production from waste and nonsalable date palm (Phoenix dactylifera L.) fruits: Potentials and challenges," *Sustainability,* vol. 15, p. 2937, 2023.

[20] N. K. Alqahtani, S. A. Ali, and T. M. Alnemr, "Quality preservation of date palm (Phoenix dactylifera L.) fruits at the Khalal stage: a review on current challenges, preservation methods, and future trends," *Frontiers in Sustainable Food Systems,* vol. 9, p. 1558985, 2025.

[21] A. J. Subhash, G. B. Bamigbade, and M. Ayyash, "Current insights into date by-product valorization for sustainable food industries and technology," *Sustainable Food Technology,* vol. 2, pp. 331-361, 2024.

[22] H. N. Dhakal, S. H. Khan, I. A. Alnaser, M. R. Karim, A. Saifullah, and Z. Zhang, "Potential of date palm fibers (DPFs) as a sustainable reinforcement for bio-composites and its property enhancement for key applications: a review," *Macromolecular Materials and Engineering,* vol. 309, p. 2400081, 2024.

[23] C. Fragassa, F. Vannucchi de Camargo, and C. Santulli, "Sustainable biocomposites: Harnessing the potential of waste seed-based fillers in eco-friendly materials," *Sustainability,* vol. 16, p. 1526, 2024.

[24] A. E. Ali, M. Gronfula, and G. Abdel-Gaber, "Reinforcing Polymers with Date Palm Seeds: A Path to Greener Composites–A Review," *SVU-International Journal of Engineering Sciences and Applications,* vol. 6, pp. 1-16, 2025.

[25] W. Marzouk, F. Bettaieb, R. Khiari, and H. Majdoub, "Composite materials based on low-density polyethylene loaded with date pits: Mechanical and thermal characterizations," *Journal of Thermoplastic Composite Materials,* vol. 30, pp. 1200-1216, 2017.

[26] L. Herzallah, F. Mansour, A. Abuarra, D. Hara, R. Abdallah, and A. Juaidi, "Experimental and economic analysis to explore the potential of managing date palm waste to generate energy for heating applications," *Environmental Development,* vol. 54, p. 101171, 2025.

[27] M. Talhami, A. H. M. Kashem, K. A. Alkhamri, O. Albatarni, M. I. Thaher, P. Das, *et al.*, "Sustainable and low-cost protic ionic liquid-based recovery of oil from agricultural wastes “date pits” for biofuel production," *Resources, Conservation & Recycling Advances,* vol. 25, p. 200246, 2025.